

## Tunneling dynamics of excitons in random semiconductor alloys

Alexander Müller\* and Marius Grundmann

*Institute of Experimental Physics II, University of Leipzig, Linnéstraße 5, 04103 Leipzig, Germany*

(Received 31 January 2012; revised manuscript received 2 January 2013; published 28 January 2013)

An analytical model describing the low-temperature tunneling dynamics of excitons in disordered systems is proposed, reproducing the time-resolved photoluminescence (TRPL) line shape and the temporal red-shift of the TRPL maximum of localized excitons in detail. Assuming a Gaussian energy distribution of the localized states, the observed asymmetric spectral line shape can be interpreted as the distribution of the lowest states within a certain tunneling volume. Using (Mg,Zn)O and Cd(S,Se) as model systems, the number of reachable states is determined from the time dependence of the photoluminescence signal and the density of localized states is estimated. For (Mg,Zn)O, we also reveal the exciton capture at donors and its influence on the TRPL transients.

DOI: [10.1103/PhysRevB.87.035134](https://doi.org/10.1103/PhysRevB.87.035134)

PACS number(s): 71.23.-k, 71.35.-y, 71.55.Jv, 78.47.jd

In order to interpret the luminescence of semiconductor alloys, the knowledge of the emission line shape and a thorough understanding of the underlying mechanisms are of crucial importance. Several empirical and physically motivated models reproducing the photoluminescence (PL) line shape of disordered solids can be found in literature. A simple Gaussian line shape<sup>1</sup> is valid if the recombination is much faster than the relaxation into local potential minima. At low temperatures, however, excitons preferentially occupy low-energy states. While an occupation probability according to a Maxwell-Boltzmann distribution with some effective temperature  $T^*$  only explains a red-shift of the Gaussian, more sophisticated models often predict asymmetric PL line shapes.<sup>2-6</sup> A model taking into account the relaxation into low-energy states was proposed by Schubert and Tsang,<sup>4</sup> however, only applied to time-integrated PL spectra. Tunneling between different localized states was handled quantum mechanically by Cohen and Sturge<sup>2</sup> to explain sidebands of the longitudinal optical (LO) phonon emission lines. For elevated temperatures, a thermal activation into delocalized states above the mobility edge was suggested by Oueslati *et al.*<sup>3</sup> and applied to time-resolved spectra by Gourdon and Lavallard.<sup>7</sup> Using a Monte Carlo simulation, an asymmetric line shape was also found for excitons within quantum wells.<sup>6</sup>

In this paper, we present an analytical tunneling model for semiconductor alloys. Taking into account that the spatially random distribution of the localized states constrains the carrier relaxation into lower potential minima, the asymmetric line shape of the low-temperature time-resolved PL (TRPL) spectra as well as the red-shift of the luminescence maximum over time are reproduced by varying only a single time-dependent parameter. This enables us to precisely model the time-delayed spectra of (Mg,Zn)O thin films over three orders of magnitude with a total dynamic range of six orders of magnitude. In contrast to most other models, no prior assumptions on microscopic parameters such as an energy-dependent exciton relaxation time constant<sup>2-4</sup> or energy-dependent transition rates<sup>2</sup> are necessary.

For low temperatures, most carriers relax into local potential minima within a few picoseconds.<sup>8</sup> As the thermal energy does not suffice to overcome the potential barriers, lower-lying localized states are reached only by phonon-assisted tunneling.<sup>2,7,9</sup> Near the excitonic band gap, the energy density of the localized states can often be approximated by a Gaussian

distribution.<sup>1</sup> Assuming that an exciton can reach  $k$  different localized states, it will most probably relax into the lowest of these. The resulting distribution of the smallest out of  $k$  Gaussian random numbers is<sup>10</sup>

$$p_k(y) = k[1 - F(y)]^{k-1} f(y) = k \left( 1 - \frac{\text{erf}(y/\sqrt{2}) + 1}{2} \right)^{k-1} \frac{\exp(-\frac{1}{2}y^2)}{\sqrt{2\pi}}, \quad (1)$$

where  $f(y)$  is the normal distribution and  $F(y)$  is the corresponding cumulative distribution.

Taking into account that the localized states are randomly distributed within the crystal with an average density  $n$ , the number of reachable states within a certain tunneling volume  $V_t$  follows a Poisson distribution  $N^k e^{-N}/k!$  with the expectation value  $N = nV_t$ . To calculate the occupation probability of the localized states, Eq. (1) is summed over all  $k \geq 0$ , leading to

$$p_N(y) = \frac{N}{\sqrt{2\pi}} \exp\left(-N \frac{\text{erf}(y/\sqrt{2}) + 1}{2} - \frac{y^2}{2}\right). \quad (2)$$

As Eq. (1) vanishes for  $k = 0$ , Eq. (2) has to be normalized by  $(1 - e^{-N})^{-1}$ . The position of the maximum of Eq. (2) is given by

$$y_{\max}(N) = -\frac{N}{2\sqrt{\pi}} \exp\left[-\frac{1}{2}W\left(\frac{N^2}{2\pi}\right)\right], \quad (3)$$

$W(z)$  being the Lambert W function.

Alloys such as  $\text{Mg}_x\text{Zn}_{1-x}\text{O}$  often show a nonexponential luminescence decay<sup>11</sup> attributed to a broad distribution of radiative lifetimes for different localized states.<sup>12</sup> Assuming that this distribution does not strongly correlate with the transition energy, the PL line shape can be derived from Eq. (2) by substituting  $y = \frac{E-E_0}{\sigma}$ . Here,  $E_0$  is the mean exciton transition energy and  $\sigma$  is the standard deviation determining the spectral linewidth of the distribution.

For excitons below the mobility edge, the probability of presence decreases approximately exponentially as a function of distance from the center of mass.<sup>13</sup> Therefore, the wavefunction overlap and consecutively the tunneling probability approximately decrease by a factor  $e$  when increasing the distance between an initial state and a prospective target state by the tunneling length  $r_{t,0}$ . On average, the time to reach the

more distant target state increases by the factor  $e$ , defining a time-dependent tunneling distance

$$r_t(t) = r_{t,0} \ln \left( \frac{t}{t_0} \right). \quad (4)$$

As simplification, we neglect that the extension of the wave function depends on the localization energy as well as the concrete potential environment around the localized state. The strongest variations are expected for states energetically near the mobility edge. However, as most excitons rapidly relax into local potential minima well below the mobility edge, only a slow variation of  $r_{t,0}$  is expected while the excitons reach energetically lower states by tunneling. Therefore, we assume that the tunneling length can be approximated by some constant average.

Statistically, within the time  $t$  an exciton can reach all states inside the volume  $V_t(t) = \frac{4}{3}\pi r_t^3(t)$ , determining the average number

$$N(t) = n \times \frac{4}{3}\pi r_t^3(t) = c \left( \ln \frac{t}{t_0} \right)^3 \quad (5)$$

of reachable states and the time-dependent emission maximum. For convenience, we define  $c := n \times \frac{4}{3}\pi r_{t,0}^3$ . As  $r_t(t_0) = 0$  (by definition), the time  $t_0$  has no direct physical meaning. Instead, it can be interpreted by means of an offset radius within which all states can be reached during the thermalization of an exciton.

It shall be noted that Eq. (2) is identical to the line shape proposed by Schubert and Tsang<sup>4</sup> for time-integrated PL spectra. The authors assume that the exciton relaxation depends on the total number of low-energy states and a given capture time constant  $\tau_c$ , not taking into account the spatial distribution of the potential minima. A linear increase of  $N \cong t/\tau_c$  was concluded from this mean-field approach, significantly overestimating the experimentally observed red-shift over time.

To verify our model, we apply it to the time-delayed PL spectra of  $\text{Mg}_x\text{Zn}_{1-x}\text{O}$  thin films grown by pulsed laser deposition on a-plane sapphire substrate (experimental details given in Ref. 12). Here, the spectra were calculated from the fitted model decay functions instead of from the transient raw data. On the one hand, this enables us to investigate the fast initial luminescence dynamics otherwise masked by the instrument function of our setup. On the other hand, the usable dynamic range is increased as the signal-dependent background is removed.

To demonstrate the accuracy of the model decay functions, selected transients of an  $\text{Mg}_{0.18}\text{Zn}_{0.82}\text{O}$  thin film are shown in Fig. 1. The transients have been individually fitted by a superposition of a monoexponential decay ( $\tau = 0.75$  ns) for the fast recombination of donor-bound excitons ( $\text{D}^0\text{X}$ ) only visible for the transients measured on the low-energy side of the spectrum and a double power law describing the slow decay of excitons localized within alloy potential fluctuations (LX). The latter is defined by

$$I(t) = \frac{I_0}{(1 + t/t_1)^{\beta_1} (1 + t/t_2)^{\beta_2}} \quad (6)$$

and can be interpreted as a superposition of different decay channels with independent distributions of lifetimes (cf. Ref. 14). The initial process with the exponent  $\beta_1$  (for  $t_1 < t_2$ )

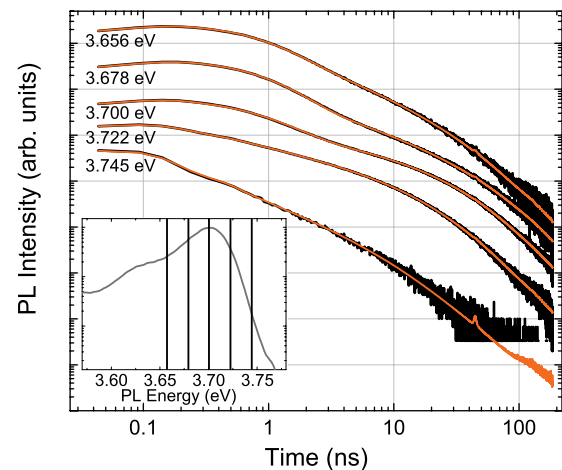


FIG. 1. (Color online) Fitted TRPL transients in a double-logarithmic plot. The spectral positions have been marked in the time-integrated PL spectrum shown in the inset.

can be explained by the tunneling dynamics as discussed below. The second exponent is attributed to the radiative decay of the excitons. The long decay times observed here can be understood by confinement effects, leading to a strong decrease of the oscillator strength of the localized states.<sup>15</sup>

The resulting time-delayed spectra for the sample are shown in Fig. 2. For all times, the main emission peak is accompanied by the corresponding 1-LO phonon replica. The PL maximum is attributed to the superposition of  $\text{D}^0\text{X}$ , dominating the spectra for short times after the laser pulse, while the LX decay determines the spectra for large times.<sup>12</sup>

Using the tunneling exciton line shape, the time-delayed spectra of the  $\text{Mg}_{0.18}\text{Zn}_{0.82}\text{O}$  sample are reproduced with great fidelity as shown in Fig. 3(b). For times larger than 3 ns, the main peak has been fitted by a single distribution according to Eq. (2), as indicated by the green curve. For smaller times, the  $\text{D}^0\text{X}$  contribution was added. In agreement with time-delayed PL spectra from samples with low Mg

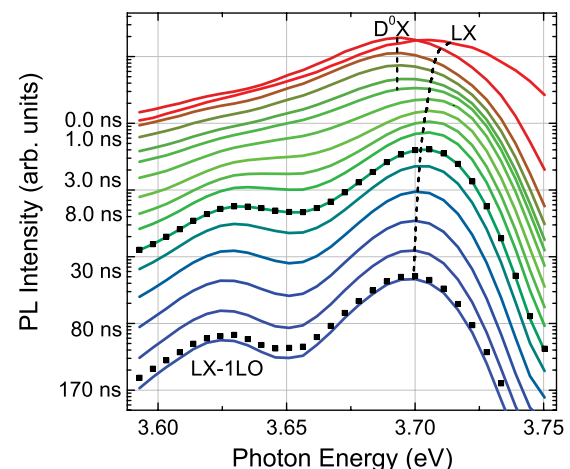


FIG. 2. (Color online) Time-delayed spectra of an  $\text{Mg}_{0.18}\text{Zn}_{0.82}\text{O}$  thin film for  $T = 5$  K. The  $\text{D}^0\text{X}$  and LX peak positions determined from the tunneling line-shape fit have been marked. For 20 and 170 ns, the spectra generated from the raw transient data are shown for comparison.

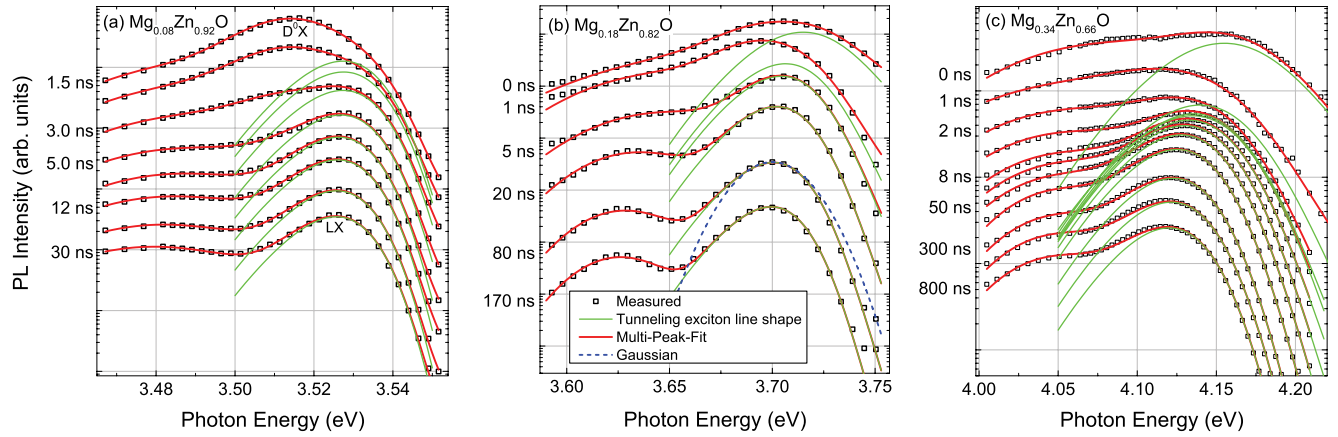


FIG. 3. (Color online) Selected time-delayed spectra ( $T = 5$  K) of three  $\text{Mg}_x\text{Zn}_{1-x}\text{O}$  thin films fitted by a sum of Eq. (2). For comparison, a Gaussian distribution is shown in (b), illustrating the asymmetry of the main peak.

content (not shown here), this can empirically be fitted using the tunneling line shape with a fixed set of parameters for all spectra. Additionally, the 1-LO phonon replicas of the main peak are approximated by Gaussian functions and included in the multipeak fit. A remarkably good agreement is found for the main emission peak, reproducing the PL line shape on the high-energy side for up to three orders of magnitude.

The parameters used to fit the time-delayed spectra are given in the upper part of Table I. The intensities of the different contributions as well as the number of reachable states  $N_{\text{LX}}$  were treated as free parameters for the individual curves. The main peak is therefore determined by three free parameters for  $t \leq 3$  ns and only two free parameters for  $t \geq 5$  ns.  $E_{\text{LX}} = (3.749 \pm 0.005)$  eV and  $\sigma_{\text{LX}} = (28 \pm 1)$  meV are in good agreement with Ref. 16. Compared to  $E_{\text{LX}}$ , the  $\text{D}^0\text{X}$  emission maximum is red-shifted by an effective donor localization energy of  $(57 \pm 5)$  meV. The value  $N_{\text{D}^0\text{X}} = 8$  indicates only a weak asymmetry of the  $\text{D}^0\text{X}$  emission band.

To prove the applicability of our model to other alloy compositions and materials, the time-delayed spectra of two additional  $\text{Mg}_x\text{Zn}_{1-x}\text{O}$  thin films [ $x = 0.08$  and  $0.34$ ; see Figs. 3(a) and 3(c)] as well as a  $\text{CdS}_{0.53}\text{Se}_{0.47}$  sample (see Fig. 4) were fitted using the tunneling exciton line shape.

TABLE I. Model parameters used to fit the time-delayed spectra and the time dependence of the average number of reachable states  $N_{\text{LX}}$ . In the bottom part of the table, the estimated tunneling length as well as the calculated density of localized exciton states are given.

Parameter	$\text{Mg}_x\text{Zn}_{1-x}\text{O}$			$\text{CdS}_x\text{Se}_{1-x}$
	$x = 0.08$	$x = 0.18$	$x = 0.34$	$x = 0.53$
$E_{\text{LX}}$ (eV)	3.562	3.749	4.215	2.11
$\sigma$ (meV)	18	28	51	11.5
$E_{\text{D}^0\text{X}}$ (eV)	3.540	3.728	4.176	
$N_{\text{D}^0\text{X}}$	11	8	8	
$c$	$1.2 \times 10^{-3}$	$1.0 \times 10^{-3}$	$1.3 \times 10^{-3}$	$1.2 \times 10^{-2}$
$t_0$ (ns)	$2.9 \times 10^{-13}$	$1.1 \times 10^{-10}$	$1.1 \times 10^{-9}$	$2.6 \times 10^{-5}$
$r_{t,0}$ (nm)	0.55	0.45	0.35	1.0
$n$ ( $\text{cm}^{-3}$ )	$1.6 \times 10^{18}$	$2.6 \times 10^{18}$	$7.6 \times 10^{18}$	$3.0 \times 10^{18}$

Indeed, a very good agreement can be observed for the different spectra. The values of  $N_{\text{LX}}$  determined from the line-shape fits are plotted as a function of time in Fig. 5. As expected, the dependence can be modeled using Eq. (5) for all samples, determining the fit parameters given in the middle part of Table I.

The parameter  $c$  enables us to provide an estimation for the density of localized exciton states  $n = 3c/(4\pi r_{t,0}^3)$ . The tunneling length  $r_{t,0}$  can be approximated from the wavefunction attenuation within a potential barrier. On the one hand, it depends on the effective exciton mass  $M = m_e^* + m_h^*$  and, on the other hand, on the average barrier height  $(V_0 - E)$  inhibiting the transfer between the different localized states.<sup>18</sup>

$$r_{t,0} \approx \frac{1}{2}\kappa^{-1} = \frac{\hbar}{2\sqrt{2M(V_0 - E)}}. \quad (7)$$

For  $\text{Mg}_x\text{Zn}_{1-x}\text{O}$ , the effective exciton mass  $M \approx m_0$  is similar to the electron rest mass,<sup>19</sup> while the average barrier height depends on the Mg content  $x$  and can be estimated from the

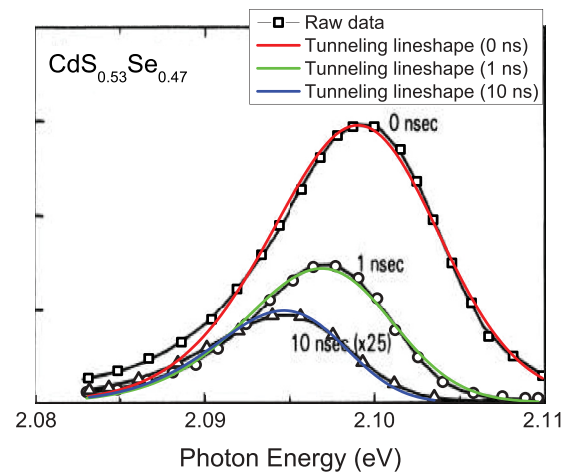


FIG. 4. (Color online) Fit of the time-delayed spectra ( $T = 2$  K) of a  $\text{CdS}_{0.53}\text{Se}_{0.47}$  sample extracted from Ref. 17 (original spectra visible in background). The deviation between measured and fitted curves visible on the low-energy side of the spectrum is attributed to the phonon replica.

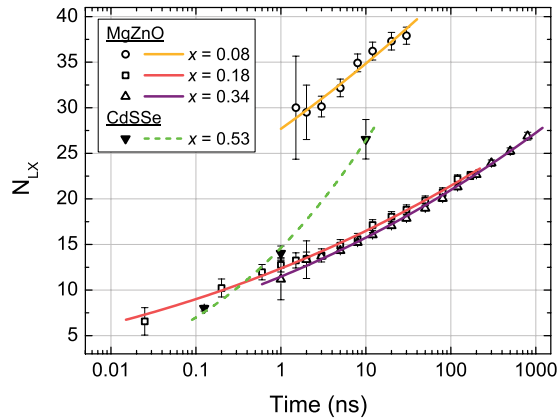


FIG. 5. (Color online) Number  $N_{LX}$  of reachable localized states determined from the line shape fits of the  $Mg_xZn_{1-x}O$  thin films and the  $CdS_{0.53}Se_{0.47}$  sample as a function of time. The dependencies were fitted by Eq. (5). Please note the logarithmic time scale.

fit of the time-delayed spectra. We use here the difference between the mean exciton transition energy  $E_{LX}$  and the luminescence maximum, leading for  $x = 0.18$  to an average barrier height  $(V_0 - E) = 46$  meV. The resulting density of exciton states is  $n = 2.6 \times 10^{18} \text{ cm}^{-3}$ . For the  $CdS_{0.53}Se_{0.47}$  sample, a significant larger tunneling length can be concluded from the smaller average barrier height and the slightly smaller exciton mass<sup>20</sup>  $M \approx 0.75m_0$ . However, due to the significantly higher slope of  $N(t)$ , a quite similar density of states can be calculated.

To further investigate the luminescence composition for the  $Mg_{0.18}Zn_{0.82}O$  alloy, the intensities of  $D^0X$  and LX are depicted in Fig. 6 as a function of time. While the LX intensity shows a fast initial decrease, indicating a capture process either at donors or at nonradiative recombination centers, the  $D^0X$  intensity initially increases. Comparing the time-integrated intensities of both components, the  $D^0X$  contribute about  $\frac{1}{3}$  to the total PL intensity of the sample. However, it has to be taken into account that the LX intensity initially decreases by a factor of 5 within the first nanosecond after the laser pulse. It can be concluded that at least 70% of the LX decay nonradiatively and only about 10% get captured at donors.

The  $D^0X$  time dependence can be modeled using an exponential decay ( $\tau = 0.77$  ns) with a rise time of 50 ps, while the initial LX intensity decrease was empirically modeled by an exponential function with a capture time of 140 ps. The discrepancy between rise and fall times can most likely be understood by the simple fit model which does not

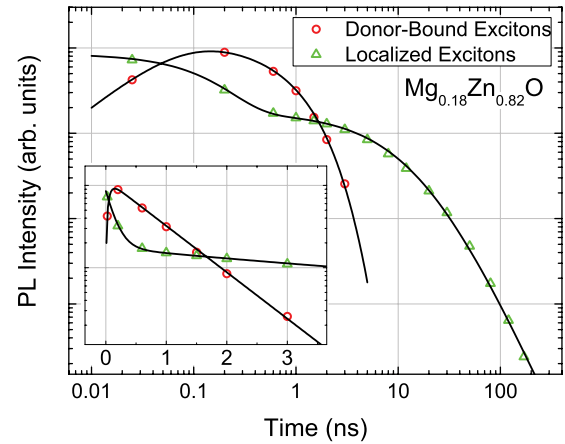


FIG. 6. (Color online) Time-dependent  $D^0X$  and LX intensities on a double-logarithmic scale. The inset magnifies the initial dynamics on a semilogarithmic scale. The solid lines are fits with a delayed exponential for the  $D^0X$  intensity and a sum of an exponential capture process and a power-law decay for the LX intensity.

include nonexponential capture processes expected due to the statistical distribution of the defects. While fast initial capture processes determine the  $D^0X$  rise time, the initial LX intensity decrease is mostly dominated by slow contributions. At long times, the LX decay follows a single power law (cf. Ref. 12), proving that the first exponent of the double power law [Eq. (6)] is attributed to the initial capture processes and the tunneling into lower-lying potential minima.

To summarize, we have presented a simple analytical model based on the random spatial arrangement of localized exciton states in various semiconductor alloys. Our model reproduces the asymmetric TRPL line shape as well as the logarithmic time-dependent red-shift of the TRPL maximum of alloy-localized excitons in various materials with great accuracy. We were able to estimate the density of localized exciton states in the alloys. Additionally, the TRPL spectra of  $(Mg,Zn)O$  were analyzed, revealing the delayed exciton capture at donors and the influence of the tunneling dynamics on the TRPL transients.

#### ACKNOWLEDGMENT

This work was supported by the Deutsche Forschungsgemeinschaft within Leipzig School of Natural Sciences—Building with Molecules and Nano-objects BuildMoNa (GS 185/1).

\*amueller@physik.uni-leipzig.de

<sup>1</sup>E. F. Schubert, E. O. Göbel, Y. Horikoshi, K. Ploog, and H. J. Queisser, *Phys. Rev. B* **30**, 813 (1984).

<sup>2</sup>E. Cohen and M. D. Sturge, *Phys. Rev. B* **25**, 3828 (1982).

<sup>3</sup>M. Oueslati, M. Zouaghi, M. E. Pistol, L. Samuelson, H. G. Grimmeiss, and M. Balkanski, *Phys. Rev. B* **32**, 8220 (1985).

<sup>4</sup>E. F. Schubert and W. T. Tsang, *Phys. Rev. B* **34**, 2991 (1986).

<sup>5</sup>D. Ouadjaout and Y. Marfaing, *Phys. Rev. B* **41**, 12096 (1990).

<sup>6</sup>E. Runge, A. Schülzgen, F. Henneberger, and R. Zimmermann, *Phys. Status Solidi B* **188**, 547 (1995).

<sup>7</sup>C. Gourdon and P. Lavallard, *Phys. Status Solidi B* **153**, 641 (1989).

<sup>8</sup>S. Shevel, R. Fischer, E. O. Göbel, G. Noll, P. Thomas, and C. Klingshirn, *J. Lumin.* **37**, 45 (1987).

<sup>9</sup>S. Permogorov, A. Reznitskii, S. Verbin, G. O. Müller, P. Flögel, and M. Nikiforova, *Phys. Status Solidi B* **113**, 589 (1982).

- <sup>10</sup>B. C. Arnold, N. Balakrishnan, H. N. Nagaraja, and H. N. Nagaraja, *A First Course in Order Statistics* (Society for Industrial Mathematics, Philadelphia, PA, 2008), p. 12.
- <sup>11</sup>A. Ohtomo, M. Kawasaki, T. Koida, K. Masubuchi, H. Koinuma, Y. Sakurai, Y. Yoshida, T. Yasuda, and Y. Segawa, *Appl. Phys. Lett.* **72**, 2466 (1998).
- <sup>12</sup>A. Müller, M. Stölzel, C. Dietrich, G. Benndorf, M. Lorenz, and M. Grundmann, *J. Appl. Phys.* **107**, 013704 (2010).
- <sup>13</sup>S. Rodt, V. Türck, R. Heitz, F. Guffarth, R. Engelhardt, U. W. Pohl, M. Straßburg, M. Dworzak, A. Hoffmann, and D. Bimberg, *Phys. Rev. B* **67**, 235327 (2003).
- <sup>14</sup>M. Berberan-Santos, E. Bodunov, and B. Valeur, *Chem. Phys.* **317**, 57 (2005).
- <sup>15</sup>M. Sugawara, *Phys. Rev. B* **51**, 10743 (1995).
- <sup>16</sup>A. Müller, G. Benndorf, S. Heitsch, C. Sturm, and M. Grundmann, *Solid State Commun.* **148**, 570 (2008).
- <sup>17</sup>J. A. Kash, A. Ron, and E. Cohen, *Phys. Rev. B* **28**, 6147 (1983).
- <sup>18</sup>Y. Ando and T. Itoh, *J. Appl. Phys.* **61**, 1497 (1987).
- <sup>19</sup>G. Coli and K. K. Bajaj, *Appl. Phys. Lett.* **78**, 2861 (2001).
- <sup>20</sup>J. W. Haus, H. S. Zhou, I. Honma, and H. Komiyama, *Phys. Rev. B* **47**, 1359 (1993).